J. Fluid Mech. (1995), *vol.* 298, *pp.* 271–285
Copyright © 1995 Cambridge University Press

Peristaltic transport of two immiscible viscous fluids in a circular tube

By ADABALA RAMACHANDRA RAO AND SRINIVASAN USHA

Department of Mathematics, Indian Institute of Science, Bangalore, India

(Received 15 December 1994 and in revised form 30 March 1995)

Peristaltic motion of two immiscible viscous incompressible fluids in a circular tube is studied in pumping and copumping ranges under long-wavelength and low-Reynolds-number assumptions. The effect of the peripheral-layer viscosity on the time-averaged flux and the mechanical efficiency is studied. The formation and growth of the trapping zone in the core and the peripheral layer are explained. It is observed that the bolus volume in the peripheral layer increases with an increase in the viscosity ratio. The limits of the time-averaged flux $\bar{Q}$ for trapping in the core are obtained. The trapping observed in the peripheral layer decreases in size with an increase in $\bar{Q}$ but never disappears. The development of the complete trapping of the core fluid by the peripheral-layer fluid with an increase in the time-averaged flux is demonstrated. The effect of peripheral-layer viscosity on the reflux layer is investigated. It is also observed that the reflux occurs in the entire pumping range for all viscosity ratios and it is absent in the entire range of copumping.

1. Introduction

'Peristalsis' is a mechanism for pumping fluid in a tube by means of a moving contractile ring around the tube, which pushes the material onward. This is analogous to constricting a distensible tube with one's fingers and moving the occlusion forward along the tube. The peristaltic wave generated along the flexible walls of the tube provides an efficient means of transport of fluids in living organisms and in industrial pumping. It is an inherent property of many syncytial smooth muscle tubes, since stimulation at any point causes a contractile ring around the tube. In general, peristalsis induces two types of fluid movements, namely propulsive and mixing. The peristaltic propulsive movement is observed in the oesophagus, the gastrointestinal tract, bileducts, the ureter and other glandular ducts throughout the body (Guyton 1986). The same principle has been adapted by engineers to pump corrosive material and fluids which are to be kept away from the pumping machinery.

Even though peristalsis is a well-known pumping phenomenon observed in biological systems for many decades, the first attempt to study the fluid mechanics of peristaltic transport is by Latham (1966). Following this experimental work, Burns & Parkes (1967) developed a mathematical model for homogeneous fluids in a channel idealized under the assumption of inertia-free motion due to an infinite train of peristaltic waves. The corresponding axisymmetric case was discussed by Barton & Raynor (1968). Later, the small-amplitude assumption was replaced by infinite wavelength by Shapiro, Jaffrin & Weinberg (1969). They studied two interesting phenomena associated with peristaltic flow, namely the material reflux and the trapping of the fluid between successive contractions for two-dimensional channels and axisymmetric tubes. The

effect of inertia and streamline curvature on peristaltic motion was investigated for a two-dimensional channel by Jaffrin (1973) and for axisymmetric tubes by Manton (1975). The effect of the intensity of the Poiseuille flow on the peristaltic motion was studied by Mittra & Prasad (1974). Liron (1976) examined the efficiency of peristaltic pumping. For a complete review of the work in the field one may refer to Jaffrin & Shapiro (1971), Rath (1980) and Srivastava & Srivastava (1984). In most of the studies at least one of the parameters, namely the amplitude ratio, the ratio of the channel width to the wavelength and the Reynolds number, is assumed to be small. Recently, Takabatake, Ayukawa & Mori (1988) in their numerical study of peristaltic transport, have relaxed all the restrictions on these parameters.

While the principle of peristaltic pumping is well understood from the analyses mentioned above, it is observed that many biological ducts undergoing peristalsis are coated with a fluid having different properties from that of the pumped fluid (Best & Taylor 1958). Shukla *et al.* (1980) were the first to attempt to study the effect of the fluid coating on peristaltic transport by considering the peristaltic motion of two immiscible Newtonian fluids in channel and axisymmetric tube geometries. They specified the interface shape, independent of the fluid viscosities, and used a trivial solution of the law of conservation of mass over one wavelength. For the two-dimensional channel, Brasseur, Corrsin & Lu (1987) have proved the invalidity of the above-mentioned analysis in the limit of infinite peripheral-layer viscosity, since the principle of mass conservation is not satisfied independently in the core and the peripheral layer across any cross-section of the tube. The influence of peripheral-layer viscosity on trapping and reflux in the pumping range (i.e. pumping from a region of lower pressure to a region of higher pressure) has been presented by Brasseur *et al.* However, the analysis of pressure-assisted peristaltic flow of a single fluid (copumping) in a two-dimensional channel by Pozrikidis (1987) shows the existence of a trapping region adjacent to the wall.

In this paper, the peristaltic transport of two fluids in an axisymmetric tube is considered. Following Brasseur *et al.* (1987), the interface, which is also a streamline, is determined from a sixth-degree equation in the core thickness. The present analysis, apart from being an adaptation of the channel geometry discussed by Brasseur *et al.* (1987) to pipe geometry, emphasizes the trapping under copumping conditions (pressure-assisted peristaltic transport) and the detachment of the trapped bolus from the centreline. The following new features are observed in our study. The non-uniqueness of the interface and its closure are observed only for a finite range of values of the time-averaged flux, $\bar{Q}$. In this range, the non-uniqueness of the interface results in the failure of the present method. Beyond this range, for sufficiently large $\bar{Q}$ the trapped bolus is observed to lie completely within the peripheral layer. The trapped bolus shrinks and moves towards the wall with a further increase in $\bar{Q}$. Further, the trapping, once established, never vanishes for any finite increase in $\bar{Q}$. The same phenomenon occurs for the case of a single fluid. Therefore, an upper bound on $\bar{Q}$ for trapping, as given by earlier authors, does not exist. The pumping characteristics such as the reflux, the trapping and the variation of time-averaged flux with pressure rise are studied as functions of the peripheral-layer fluid viscosity. The trapping phenomenon is discussed at length in both the pumping and copumping ranges. Under copumping the increase in the viscosity ratio gives rise to trapping in the peripheral layer near the wall.

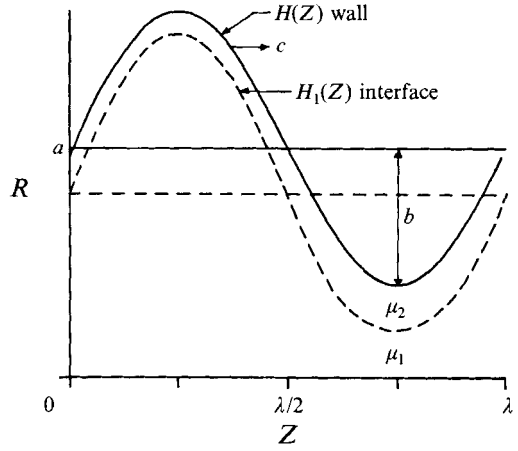

FIGURE 1. Peristaltic transport in a stationary frame of reference.

2. Mathematical formulation and solution

Consider the peristaltic transport of a bio-fluid consisting of two immiscible and incompressible fluids of different viscosities μ_1 and μ_2 occupying the core and peripheral layers in a circular tube of radius a. The axisymmetric geometry facilitates the choice of the cylindrical polar coordinate system (R, θ, Z) to study the problem. The wall deformation due to the propagation of an infinite train of peristaltic waves is given by

$$R = H(Z,t) = a + b\sin\frac{2\pi}{\lambda}(Z-ct),$$

where b is the amplitude, λ is the wavelength and c is the wave speed. The subsequent deformation of the interface separating the core and the peripheral layer is denoted by $R = H_1(Z,t)$ (figure 1) which is not known *a priori*.

2.1. *Equations of motion*

Under the assumptions that the tube length is an integral multiple of the wavelength λ and the pressure difference across the ends of the tube is a constant, the flow becomes steady in a frame (r, θ, z) moving with velocity c away from the fixed frame (R, θ, Z) (Jaffrin & Shapiro 1971) and the transformation is given by

$$r = R, \quad \theta = \theta, \quad z = Z - ct, \tag{1a}$$

$$\psi = \Psi - \tfrac{1}{2}R^2 \quad \text{and} \quad p(Z,t) = p(z). \tag{1b, c}$$

In (1*b*) ψ and Ψ are the stream functions in the moving and stationary frames respectively. The assumption of negligible surface tension on the interface makes the pressure p remain a constant in any cross-section of the tube given by z = constant. Using the non-dimensional quantities

$$\bar{r} = \frac{r}{a}, \quad \bar{z} = \frac{z}{\lambda}, \quad \bar{t} = \frac{ct}{\lambda}, \quad h = \frac{H}{a}, \quad h_1 = \frac{H_1}{a}, \quad \epsilon = \frac{b}{a}, \tag{2a–f}$$

$$\bar{\psi} = \frac{\psi}{\pi a^2 c}, \quad \bar{w} = \frac{1}{r}\frac{\partial\bar{\psi}}{\partial\bar{r}}, \quad \bar{u} = -\frac{1}{r}\frac{\partial\bar{\psi}}{\partial\bar{z}}, \tag{g–i}$$

$$\begin{aligned} \bar{\mu}_r &= 1, && 0 \leqslant \bar{r} \leqslant h_1, \\ &= \mu(=\mu_2/\mu_1), && h_1 \leqslant \bar{r} \leqslant h, \end{aligned} \tag{2j}$$

and
$$\bar{p} = \frac{a^2}{\pi\lambda\mu_1 c} p, \tag{2k}$$

where $\bar{u}$ and $\bar{w}$ are the radial and axial velocities in the wave frame, in the equations governing the motion, under the lubrication approach, we get (dropping the bars):

$$\frac{1}{r}\frac{\partial}{\partial r}\left[\mu_r r \frac{\partial}{\partial r}\left\{\frac{1}{r}\frac{\partial \psi}{\partial r}\right\}\right] = \frac{\partial p}{\partial z}, \tag{3a}$$

$$0 = \frac{\partial p}{\partial r}. \tag{3b}$$

The dimensionless boundary conditions are

$$\left.\begin{aligned} \psi &= 0 \\ \frac{\partial}{\partial r}\left(\frac{1}{r}\frac{\partial \psi}{\partial r}\right) &= 0 \end{aligned}\right\} \quad \text{at} \quad r = 0, \tag{4}$$

$$w = \frac{1}{r}\frac{\partial \psi}{\partial r} = -1 \quad \text{at} \quad r = h(z), \tag{5}$$

$$\psi = \tfrac{1}{2}q \quad \text{at} \quad r = h, \tag{6}$$

$$\psi = \tfrac{1}{2}q_1 \quad \text{at} \quad r = h_1, \tag{7}$$

where q and q_1 are the total and the core fluxes respectively across any cross-section in the wave frame. Further, the velocity and the shear stress are continuous across the interface. The peripheral-layer flux is given by $q_2 = q - q_1$. It follows from the incompressibility of the fluids and the lubrication theory that q, q_1 and q_2 are independent of z. The average non-dimensional volume flow rate over one period $T(= \lambda/c)$ of the peristaltic wave is defined as

$$\begin{aligned} \bar{Q} &= \frac{2}{T}\int_0^T \int_0^h (w+1)\, r \, \mathrm{d}t \\ &= q + \frac{1}{T}\int_0^T h^2 \, \mathrm{d}r \, \mathrm{d}t \\ &= q + 1 + \tfrac{1}{2}c^2. \end{aligned} \tag{8}$$

The streamfunction is determined using the boundary conditions mentioned earlier together with the boundary conditions at the ends of the pipe given by specifying $\bar{Q}$ or the pressure difference Δp across one wavelength.

2.2. *Solution*

Solving equation (3) together with the boundary conditions (4)–(6), we obtain the stream function in the core and the peripheral layer as

$$\psi = -\frac{r^2}{2} + \left(\frac{q+h^2}{2}\right)\frac{\mu r^2(2h_1^2 - r^2) + 2r^2(h^2 - h_1^2)}{h^4 + (\mu - 1)h_1^4}, \quad 0 \leqslant r \leqslant h_1, \tag{9a}$$

$$= -\frac{r^2}{2} + \left(\frac{q+h^2}{2}\right)\frac{\mu h_1^4 + 2h_1^2(h^2 - h_1^2) + (r^2 - h_1^2)(2h^2 - r^2 - h_1^2)}{h^4 + (\mu - 1)h_1^4}, \quad h_1 \leqslant r \leqslant h. \tag{9b}$$

The stream function for the case of a single fluid is obtained by putting $\mu = 1$ in either (9*a*) or (9*b*). The pressure gradient is obtained by using equation (9) in (3) as

$$\frac{dp}{dz} = \frac{-8\mu(q+h^2)}{h^4+(\mu-1)h_1^4}. \tag{10}$$

Integrating (10) over one wavelength, we get the pressure rise (drop) over one cycle of the wave as

$$\begin{aligned}\Delta p &= -8\mu q I_1 - 8\mu I_2 \\ &= -8\mu(\bar{Q}-1-\tfrac{1}{2}\epsilon^2) I_1 - 8\mu I_2,\end{aligned} \tag{11}$$

where $$I_1 = \int_0^1 \frac{dz}{h^4+(\mu-1)h_1^4} \quad \text{and} \quad I_2 = \int_0^1 \frac{h^2\,dz}{h^4+(\mu-1)h_1^4}.$$

The time-averaged flux at zero pressure rise is denoted by $\bar{Q}_0$ and the pressure rise required to produce zero average flow rate is denoted by Δp_0.

2.3. *The equation for the interface*

The interface is also a streamline as seen from the boundary condition (7). For a given geometry of the wave and the time-averaged flux $\bar{Q}$, the unknown interface $h_1(z)$ is solved from (9) using the boundary condition (7). Substituting (7) in (9), we get the algebraic equation governing the interface $h_1(z)$ as

$$K(h_1) = (\mu-1)h_1^6 + [(2-\mu)(q+h^2) - q_1(1-\mu)]h_1^4 - h^2(h^2+2q)h_1^2 + q_1 h^4 = 0. \tag{12}$$

Since q and q_1 are independent of z, using $h_1 = \alpha$ at $z = 0$ in (12) we get

$$q_1 = \alpha^2 \frac{[(1-\mu)\alpha^4 + (1+2q) - (2-\mu)(1+q)\alpha^2]}{1+(\mu-1)\alpha^4}. \tag{13}$$

Given $\bar{Q}$, μ and ϵ the algebraic equation (12) is solved for h_1 at every z to give the interface.

Equation (12) is cubic in h_1^2 and, therefore, can have at most three positive real roots. The interface is well defined whenever there exists a single root of h_1 in the interval $(0, h)$. It is seen that

$$K(0) = q_1 h^4 \quad \text{and} \quad K(h) = -\mu q_2 h^2. \tag{14}$$

Case (i): when $q_1, q_2 \leqslant 0$ or $q_1, q_2 \geqslant 0$ it is seen from (14) that either one root or three roots exist for a given z. Case (ii): when $q_1 < 0$, $q_2 > 0$ or $q_1 > 0$, $q_2 < 0$, either there are no roots or two roots for a given z, i.e. the interface whenever it exists is not unique. The non-existence of h_1 for some z makes it impossible to calculate Δp in terms of $\bar{Q}$ using (11), making the method inapplicable. It can be easily seen that the transition from case (i) to case (ii) occurs when $q_1 = 0$ and the reverse transition occurs when $q_2 = 0$.

3. Discussion of the results

3.1. *The interface*

The limits of $\bar{Q}$ for a non-unique interface are obtained from the equalities $q_1 = 0$ and $q_2 = 0$ in case (i) of the previous section using (8) and (13) as

$$\bar{Q}_{c1} = \frac{\epsilon^2}{2} + \frac{1+(\mu-1)\alpha^4}{2+(\mu-2)\alpha^2} \tag{15a}$$

	μ	α	0.98	0.9	0.8	0.7
(*a*)	0.01	$\bar{Q}_{c1}$	1.1581	1.0830	0.9984	0.9238
		$\bar{Q}_{c2}$	2.3733	2.0245	1.8314	1.6747
		$\bar{Q}_0$	0.8204	0.8415	0.8644	0.8803
	0.5		1.1432	1.0360	0.9446	0.8756
			13.7865	3.7166	2.3889	1.9054
			0.8871	0.8917	0.8962	*
	1		1.1419	1.0203	0.9153	0.8423
			25.4325	5.4432	2.9578	2.1408
			0.9140	0.9140	0.9140	*
	5		1.1407	0.9981	0.8531	0.7450
			118.6010	19.2557	7.5089	4.0239
			0.9309	0.9592	*	*
	10		1.1405	0.9943	0.8382	0.7139
			235.0617	36.5216	13.1978	6.3778
			0.9339	0.9731	*	*
	100		1.1404	0.9904	0.8220	0.6752
			2331.3529	347.3058	115.5978	48.7483
			0.9368	*	*	*
(*b*)	0.01	$\bar{Q}_{c1}$	1.2901	1.2230	1.1304	1.0637
		$\bar{Q}_{c2}$	2.5133	2.1645	1.9714	1.8147
		$\bar{Q}_0$	1.2108	*	*	*
	0.5		1.2832	1.1760	1.0846	1.0156
			13.9265	3.0566	2.5200	2.0454
			1.2473	*	*	*
	1		1.2819	1.1603	1.0053	0.9823
			25.5725	5.5832	3.0978	2.2807
			1.2539	*	*	*
	5		1.2807	1.1382	0.9931	0.8850
			118.7410	19.3957	7.6489	4.1639
			1.2654	*	*	*
	10		1.2805	1.1343	0.9782	0.8539
			235.2017	36.6616	13.3378	6.5178
			1.2687	*	*	*
	100		1.2804	1.1304	0.9620	0.8152
			2331.4929	347.4458	115.7378	48.8883
			*	*	*	*

TABLE 1. Limiting fluxes $\bar{Q}_{c1}$ and $\bar{Q}_{c2}$ for interface closure: (*a*) $\epsilon = 0.6$, (*b*) $\epsilon = 0.8$.

and

$$\bar{Q}_{c2} = \frac{\epsilon^2}{2} + \frac{1+(\mu-1)\alpha^4}{(1-\alpha^2)}, \tag{15b}$$

respectively. It is easily seen that $\bar{Q}_{c2} - \bar{Q}_{c1} \geqslant 0$ for all $0 < \alpha \leqslant 1$ and $\mu > 0$. The limits $\bar{Q}_{c1}$ and $\bar{Q}_{c2}$ and the time-averaged flux for zero pressure rise $\bar{Q}_0$ are given in table 1(*a*) for $\epsilon = 0.6$ and in table 1(*b*) for $\epsilon = 0.8$ for various values of μ and α.

From table 1, we observe that for a given $0 < \alpha < 1$, $\bar{Q}_{c1}$ and $\bar{Q}_{c2}$ are monotonically decreasing and increasing functions of μ respectively and hence the range of non-unique roots for the interface (i.e. $\bar{Q}_{c1} - \bar{Q}_{c2}$) increases with an increase in the viscosity ratio μ. Further, the time-averaged flux $\bar{Q}_0$ is found to increase with an increase in the viscosity ratio and ϵ which is similar to the observation by Brasseur *et al.* (1987) for a channel geometry. It is also seen that $\bar{Q}_0$ decreases with an increase in α. The calculation of $\bar{Q}_0$ is not possible whenever $\bar{Q}_{c1}$ lies in the pumping range ($\Delta p \geqslant 0$) owing to the inability to use equation (11), as indicated in the table with asterisks. It is

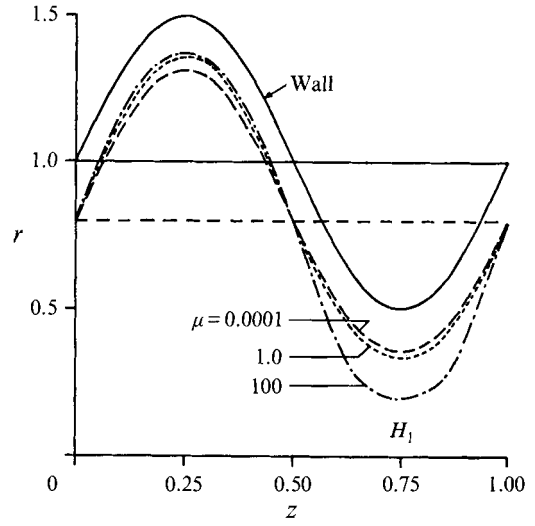

FIGURE 2. The shape of the interface for $\alpha = 0.8$, $\bar{Q} = 0.1$, $\epsilon = 0.5$ and for different viscosity ratios.

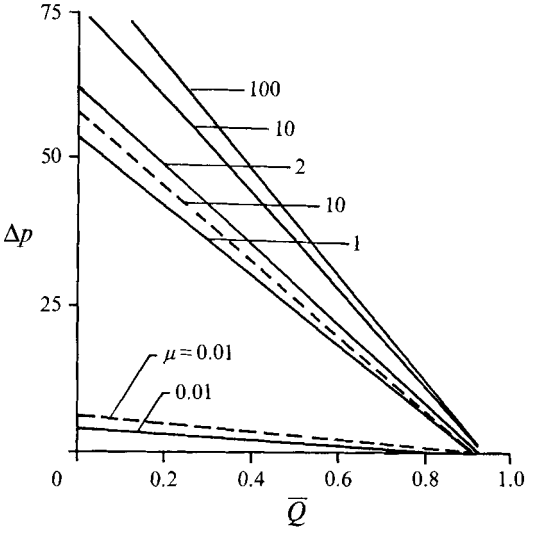

FIGURE 3. The variation of $\bar{Q}$ with Δp for different μ with $\epsilon = 0.6$ and $\alpha = 0.98$: ------, results of Shukla *et al.*; ——, results of the present model.

interesting to observe that $\bar{Q}_{c2}$ always lies in the copumping range ($\Delta p < 0$) as the corresponding flow rate in the wave frame is positive. The choice of the parameters μ, α and ϵ in the present analysis is more restricted for both pumping and copumping than the two-dimensional case discussed by Brasseur *et al.* (1987). Table 1 gives the guidelines for choosing appropriate parameters to get a well-defined interface in both the pumping and copumping ranges.

The shape of the interface for different viscosity ratios with $\alpha = 0.8$, $\epsilon = 0.5$ and $\bar{Q} = 0.1$ ($< \bar{Q}_{c1}$) is depicted in figure 2. The variation of the interface shape is similar to the channel geometry studied by Brasseur *et al.* (1987), i.e. low viscosity gives rise to a thicker peripheral layer in the dilated region. The uniform sinusoidal interface shape given by Shukla *et al.* (1980) is never obtained. The variation of pressure rise

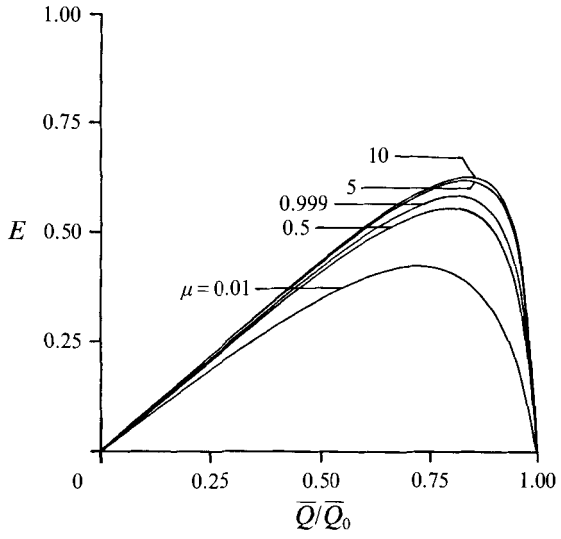

FIGURE 4. Variation of mechanical efficiency with $\bar{Q}$ for different μ with $\epsilon = 0.6$ and $\alpha = 0.98$.

with time-averaged flux is calculated from equation (11) for different viscosity ratios and is shown in figure 3. We observe that the larger the viscosity ratio the greater the pressure rise against which the pump works. The sensitivity of the time-averaged flux to the pressure rise decreases with an increase in the viscosity ratio. The disparity between the present results and those of Shukla *et al.* (1980) is small for small μ and significant for large μ.

Another important physical quantity of interest in pumping performance is the mechanical efficiency of pumping given by

$$E = \frac{\bar{Q}\Delta p}{\frac{1}{T}\int_0^T \int_0^\lambda 2hp \frac{\mathrm{d}h}{\mathrm{d}t}\mathrm{d}Z\,\mathrm{d}t} = \frac{\bar{Q}\Delta p}{\Delta p(1+\frac{1}{2}\epsilon^2)+8\mu q I_2+8\mu I_3},$$

where

$$I_3 = \int_0^1 \frac{h^4\,\mathrm{d}z}{h^4+(\mu-1)h_1^4}.$$

The numerator denotes the average rate of work done by the fluid over one wavelength against the pressure rise and the denominator denotes the average rate of work done by the wall over one wavelength, both being averaged over one period of the wave. The mechanical efficiency E as a function of $\bar{Q}$ is plotted in figure 4 for different μ and it is observed that the pumping efficiency is greater for larger viscosity ratio. This is obvious since the peristaltic motion in the pumping range depends on the viscous forces originating from the wall.

3.2. *Reflux phenomena*

Reflux is defined as the presence of some fluid particles whose mean motion over one cycle is against the net pumping direction. Jaffrin & Shapiro (1971) have emphasized that this phenomenon should be studied in the fixed frame of reference using the Lagrangian method. Following Jaffrin & Shapiro (1971), Q_ψ is defined as the dimensionless volume flow rate between the axis of the tube and a streamline ψ = constant in the fixed frame and, hence,

$$Q_\psi = 2\psi + r^2 = 2\Psi. \tag{16}$$

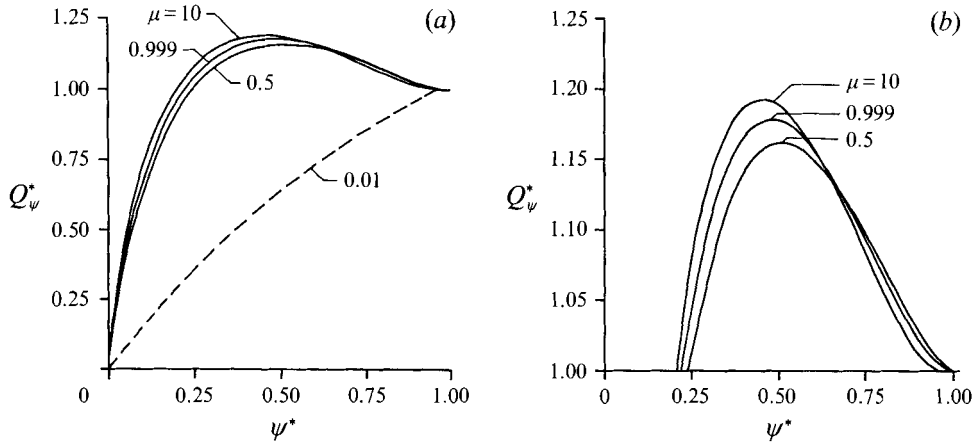

FIGURE 5. (*a*) $\bar{Q}^*_\psi$ versus ψ^* with fixed $\bar{Q}$ and different μ. (*b*) Magnification of 5(*a*) for $\bar{Q}_\psi > \bar{Q}$.

Averaging (16) over one period of the wave, we get

$$\bar{Q}_\psi = 2\psi + \int_0^1 r^2(\psi, z)\,\mathrm{d}z. \tag{17}$$

Now define $\bar{Q}^*_\psi = \bar{Q}_\psi/\bar{Q}$, $\psi^* = 2\psi/q$, where $\bar{Q}$ and q are the values of $\bar{Q}_\psi$ and ψ at the wall. Figure 5 shows the variation of $\bar{Q}^*_\psi$ as a function of ψ^* for a fixed value of $\bar{Q}$. If $\bar{Q}^*_\psi$ increases with an increase in ψ^* then the motion of the particles is always in the pumping direction. Shapiro *et al.* (1969) have shown for a single fluid that a reflux layer exists near the wall whenever $\bar{Q}^*_\psi$ increases to a value greater than unity and decreases to unity at the wall. From figure 5(*a*) the graph corresponding to $\mu = 0.01$ shows that $\bar{Q}^*_\psi$ increases steadily with an increase in ψ^* and attains unity only at the wall, which implies the absence of reflux. For $\mu = 0.5$, 0.999, and 10, there is a reflux layer adjacent to the wall as seen from figure 5(*b*) and the reflux zone widens with an increase in μ. In order to obtain the limits on $\bar{Q}$ for reflux, we expand r in powers of $\psi - \frac{1}{2}q$, using equation (9*b*), for a given value of ψ near the wall. The first two terms are considered, the higher-order terms being negligible. Using this expression for r in (9), the reflux condition $\bar{Q}^*_\psi \geqslant 1$ is obtained as

$$-\int_0^1 \frac{8\mu(q+h^2)\,\mathrm{d}z}{h^4 + (\mu-1)h_1^4} \geqslant 0, \tag{18}$$

which implies that $\Delta p \geqslant 0$. This shows that the reflux occurs in the entire pumping range and is absent in the entire copumping range irrespective of the viscosity ratio, unlike the case of channel geometry.

3.3. *Trapping*

Following Brasseur *et al.* (1987), the trapping limits are given by the values of $\bar{Q}$ when $\psi = 0$ at some r other than the centreline $r = 0$. First, we restrict our analysis to the case when the interface between the two fluids lies outside the trapping region. Hence, we choose equation (9*a*) to determine the trapping limits. By setting $\psi = 0$, we get

$$r^2 = \frac{h^2(h^2+2q) - (\mu-1)h_1^2[h^2 - 2(q+h^2)]}{\mu(q+h^2)}. \tag{19}$$

When trapping occurs, $r^2 > 0$ for some z. Therefore, both the numerator and the denominator should be of the same sign. Since the denominator attains maximum and

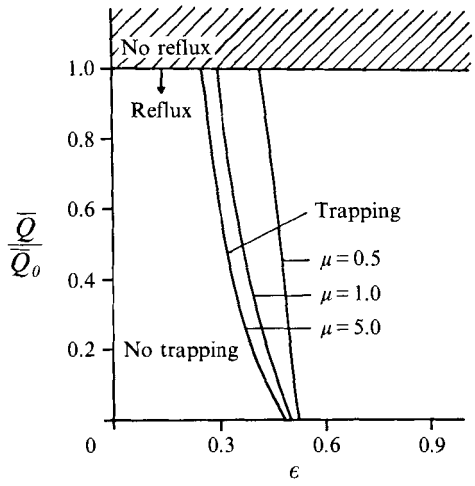

FIGURE 6. Trapping and reflux limits for different μ with $\alpha = 0.98$.

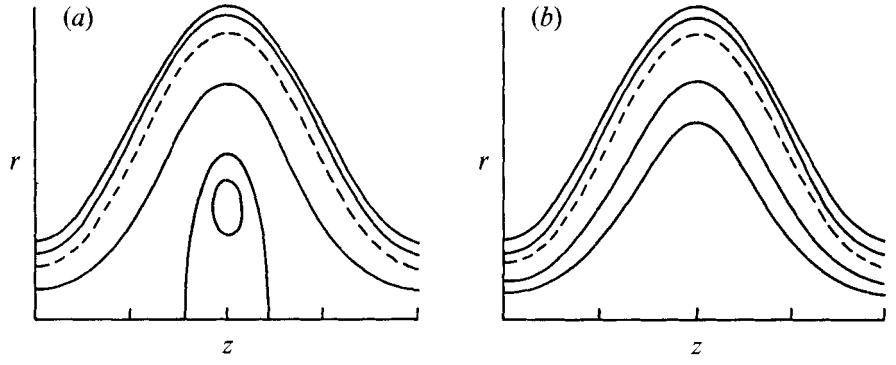

FIGURE 7. Streamlines in the wave frame for pumping with $\alpha = 0.8$, $\epsilon = 0.6$, $\mu = 0.5$. (*a*) $\bar{Q} = 0.5$, trapping; (*b*) $\bar{Q} = 0.01$, no trapping. The dashed line shows the interface.

minimum values at $z = \frac{1}{4}$ and $\frac{3}{4}$ respectively, we get the following lower and the upper trapping limits for $\bar{Q}$ for trapping attached to the centreline:

$$\bar{Q}^- = \frac{(\mu-1)h_{1max}^2[h_{1max}^2 - \epsilon(4+\epsilon)] + (1+\epsilon^2)(1-2\epsilon)}{2[h_{1max}^4(\mu-1) + (1+\epsilon)^2]}, \tag{20}$$

$$\bar{Q}^+ = \frac{(\mu-1)h_{1min}^2[h_{1min}^2 + \epsilon(4-\epsilon)] + (1-\epsilon^2)(1+2\epsilon)}{2[h_{1min}^4(\mu-1) + (1-\epsilon)^2]}. \tag{21}$$

As h_1 is a function of $\bar{Q}$, these equations are solved for the trapping limits iteratively. Figure 6 shows the reflux and trapping limits for different viscosity ratios. The area of the trapping region increases with the viscosity ratio. It is obvious that in the limit of total occlusion, the fluid is trapped irrespective of the viscosity ratio. Reflux occurs in the entire domain $0 \leqslant \bar{Q}/\bar{Q}_0 \leqslant 1$ for all values of μ, α, and ϵ and is indicated in figure 6. The streamlines in the wave frame for pumping with $\alpha = 0.8$, $\epsilon = 0.6$, and $\mu = 0.5$ for different values of $\bar{Q}$ are shown in figure 7. From figure 7(*b*) it is observed that there is no trapping for $\bar{Q} = 0.01$. When $\bar{Q}$ is increased, i.e. for $\bar{Q} = 0.5$, trapping occurs as shown in figure 7(*a*).

In the copumping range, the streamlines shown in figure 8 indicate that for $\bar{Q} = 0.94$ ($< \bar{Q}_{c1}$), a trapping region exists in the core layer and the interface lies completely

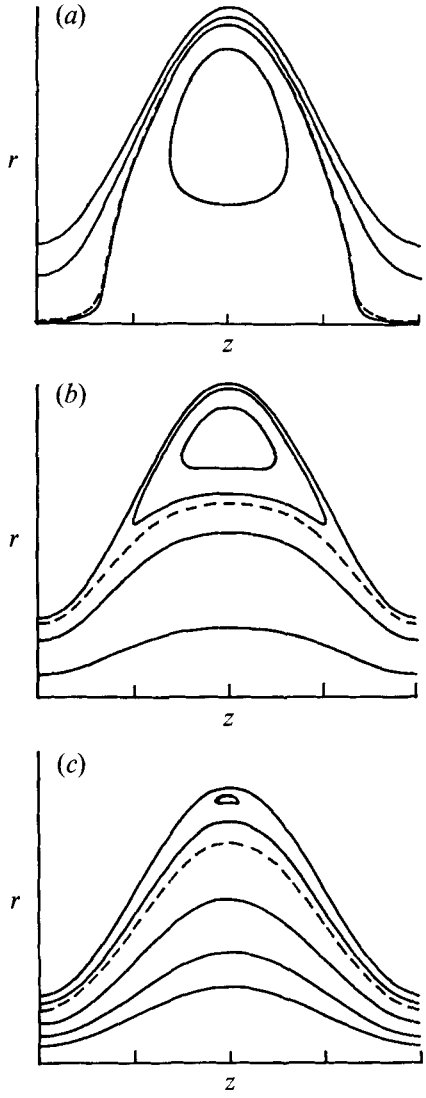

FIGURE 8. Streamlines in the wave frame for copumping with $\alpha = 0.8$, $\epsilon = 0.6$, $\mu = 0.5$. (*a*) $\bar{Q} = 0.94$, trapping in the core layer; (*b*) $\bar{Q} = 15.0$, trapping in the peripheral layer; (*c*) $\bar{Q} = 50$, trapping.

above the trapping region. For fluxes between $\bar{Q}_{c1}$ and $\bar{Q}_{c2}$, there is a possibility of the interface getting trapped, which is beyond the scope of the present study. For a sufficiently large value of $\bar{Q}$, one of the streamlines splits at the trough of the wavy wall and the trapping zone shifts to the peripheral layer. Figure 8(*b*) depicts the trapping region for $\bar{Q} = 15\,(> \bar{Q}_{c2})$ in the peripheral layer. Here, the interface is well defined and lies completely below the trapping zone. When $\bar{Q} = 50$, the trapping zone moves closer to the wall and reduces in size as seen in figure 8(*c*). When $\bar{Q} > \bar{Q}_{c2}$, q_1 and q_2 are positive and $q > q_1$, showing that the stream function increases from $q_1/2$, the value at the interface, to $q/2$, the value at the wall. But, as $\partial\psi/\partial r < 0$ at the wall, ψ attains a maximum value at some r in (h_1, h), given by

$$r^2 = h^2 - \frac{h^4 + (\mu - 1)h_1^4}{2(q + h^2)}, \tag{22}$$

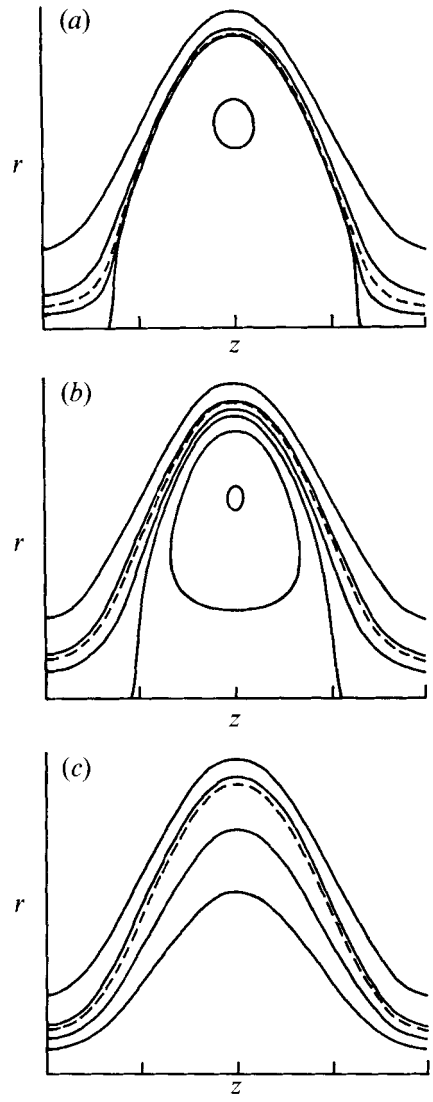

FIGURE 9. Streamlines in the wave frame for pumping with $\bar{Q} = 0.6$, $\alpha = 0.8$, $\epsilon = 0.6$. (*a*) $\mu = 5.0$ and (*b*) $\mu = 0.5$, trapping in the core layer; (*c*) $\mu = 0.01$, no trapping in the core layer.

and the corresponding maximum value of ψ is given by

$$\psi_{max}(z) = \frac{q}{2} + \frac{h^4 + (\mu - 1)h_1^4}{8(q + h^2)}. \tag{23}$$

It is easily seen that $\psi_{max}(0.75) \leqslant \psi_{max}(1.25)$ and the equality is achieved only when $\bar{Q} \to \infty$. This clearly shows that the trapping zone is always present for all values of μ and for any finite $\bar{Q} > \bar{Q}^-$. But, it decreases in size with an increase in $\bar{Q}$ and reduces to a point on the wall when $\bar{Q} \to \infty$, indicating that there is no upper limit of $\bar{Q}$ for trapping, contrary to the prediction of Shapiro *et al.* (1969).

The formation and the growth of the trapping zone in the core layer for different values of μ is shown in figure 9 for a fixed $\bar{Q} = 0.6$, $\alpha = 0.8$ and $\epsilon = 0.6$. There is no

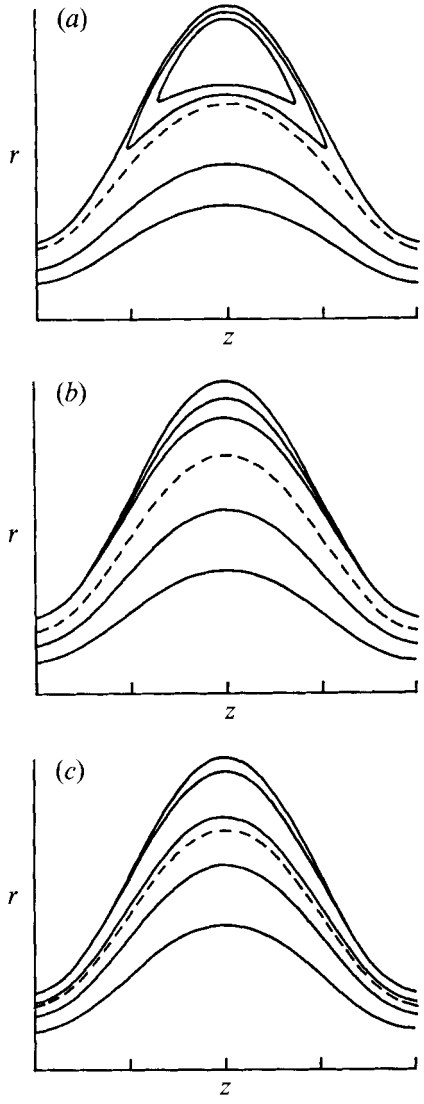

FIGURE 10. Streamlines in the waveframe for copumping with $\bar{Q} = 8.0$, $\alpha = 0.8$, $\epsilon = 0.6$. (*a*) $\mu = 5.0$, trapping in the peripheral layer; (*b*) $\mu = 0.5$ and (*c*) $\mu = 0.01$, no trapping in the core layer.

trapping for the small value of $\mu = 0.01$ as seen from figure 9(*c*). As we increase μ trapping develops and the bolus volume increases (figure 9(*b*, *a*)). The formation and growth of the trapping zone in the peripheral layer with increasing μ for $\bar{Q} = 8.0$ are shown in figure 10. The trapping is not significant when $\mu = 0.01$ (figure 10*c*) and the growth of the bolus with an increase in μ, as observed in the case of pumping, is seen from figures 10(*b*) and 10(*a*). As $\bar{Q}_{c2} - \bar{Q}_{c1}$ is an increasing function of μ, there exists a μ beyond which a given value $\bar{Q}$ would lie in the range $(\bar{Q}_{c1}, \bar{Q}_{c2})$. Hence, irrespective of whether there is pumping or copumping, for a fixed $\bar{Q}$ trapping grows with an increase in μ resulting in the trapping of the interface, and the interface remains closed for any further increase in μ.

The study of the bolus transport of fluid of one viscosity trapped within a fluid of different viscosity needs reformulation owing to the inability to determine the stream

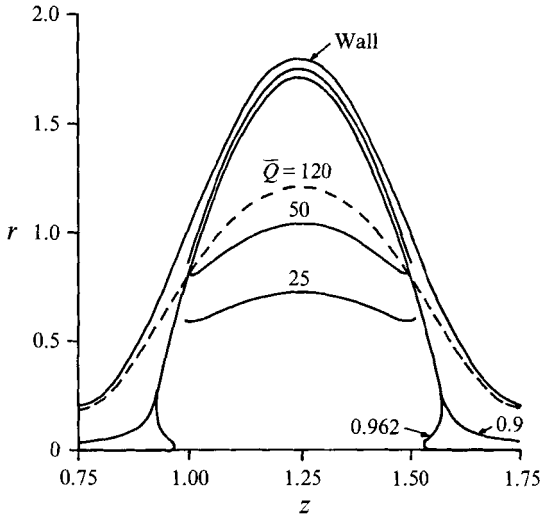

FIGURE 11. The shape of the interface for $\alpha = 0.8$, $\mu = 0.5$, $\epsilon = 0.8$ and for different $\bar{Q}$.

function given in (9*a*, *b*) for all z. However, the development of the trapping of the interface with an increase in $\bar{Q}$ can be studied using (12) and is shown in figure 11 for $\mu = 0.5$, $\epsilon = 0.8$, and $\alpha = 0.8$. When $\bar{Q} = 0.9$, the interface is unique and the trapping region, if it exists, is confined to the core layer. For sufficiently large $\bar{Q}$, there are three roots for the interface equation (12) for some z, indicating the folding of the interface. For a higher value of $\bar{Q}$, the interface appears to be trapped inside the bolus near the centreline. The volume of the core fluid trapped inside the closed interface decreases as the trapping zone detaches from the centreline and moves towards the trough of the wavy wall as seen from the graph for $\bar{Q} = 50$. When $\bar{Q} = 120 > \bar{Q}_{c2}$, a unique interface is seen once again, and in this case the trapping zone moves completely to the peripheral layer. Hence, it appears that the upper limit of trapping in the core layer and the lower limit of trapping in the peripheral layer always lie in the range $(\bar{Q}_{c1}, \bar{Q}_{c2})$.

The authors thank the referees for their valuable suggestions.

REFERENCES

BARTON, C. & RAYNOR, S. 1968 Peristaltic flow in tubes. *Bull. Math. Biophys.* **30**, 663–680.

BEST, C. H. & TAYLOR, N. B. 1958 *The Living Body*. Chapman and Hall Ltd.

BRASSEUR, J. G., CORRSIN, S. & LU, N. Q. 1987 The influence of a peripheral layer of different viscosity on peristaltic pumping with Newtonian fluid. *J. Fluid Mech.* **174**, 495–519.

BURNS, J. C. & PARKES, T. 1967 Peristaltic motion. *J. Fluid Mech.* **29**, 731–743.

GUYTON, A. C. 1986 *Text Book of Medical Physiology*. Philadelphia: Saunders Co.

JAFFRIN, M. Y. 1973 Inertia and streamline curvature effects on peristaltic pumping. *Intl J. Engng Sci.* **11**, 681–699.

JAFFRIN, M. Y. & SHAPIRO, A. H. 1971 Peristaltic pumping. *Ann. Rev. Fluid Mech.* **3**, 13–36.

LATHAM, T. W. 1966 Fluid motions in a peristaltic pump. MS thesis, MIT.

LIRON, N. 1976 On peristaltic flow and its efficiency. *Bull. Math. Biol.* **38**, 573–596.

MANTON, M. J. 1975 Long wavelength peristaltic pumping at low Reynolds number. *J. Fluid Mech.* **68**, 467–476.

MITTRA, T. K. & PRASAD, S. N. 1974 Interaction of peristaltic motion with poiseuille flow. *Bull. Math. Biol.* **36**, 127–141.

POZRIKIDIS, C. 1987 A study of peristaltic flow. *J. Fluid Mech.* **180**, 515–527.

RATH, H. J. 1980 *Peristaltische Strömungen.* Springer.

SHAPIRO, A. H., JAFFRIN, M. Y. & WIENBERG, S. L. 1969 Peristaltic pumping with long wavelengths at low Reynolds number. *J. Fluid Mech.* **37**, 799–825.

SHUKLA, J. B., PARIHAR, R. S., RAO, B. R. P. & GUPTA, S. P. 1980 Effects of peripheral-layer viscosity on peristaltic transport of a biofluid. *J. Fluid Mech.* **97**, 225–237.

SRIVASTAVA, L. M. & SRIVASTAVA, V. P. 1984 Peristaltic transport of blood: Casson model II. *J. Biomech.* **17**, 821–829.

TAKABATAKE, S., AYUKAWA, K. & MORI, A. 1988 Peristaltic pumping in circular cylindrical tubes: A numerical study of fluid transport and its efficiency. *J. Fluid Mech.* **193**, 267–283.